Geochemistry Geophysics Geosystems G3
AN ELECTRONIC JOURNAL OF THE EARTH SCIENCES
Published by AGU and the Geochemical Society

Article
Volume 7, Number 12
29 December 2006
Q12N08, doi:10.1029/2006GC001353
ISSN: 1525-2027

Phase lag between Intertropical Convergence Zone migration and subtropical monsoon onset over the northwestern Indian Ocean during Marine Isotopic Substage 6.5 (MIS 6.5)

B. Malaizé and C. Joly
Université Bordeaux I, DGO-UMR CNRS 5805 EPOC, Avenue des Facultés, F-33405 Talence, France (b.malaize@epoc.u-bordeaux1.fr)

M.-T. Vénec-Peyré
CNRS, UMR5143, F-75005 Paris, France

MNHN, UMR5143, F-75005 Paris, France

Université Pierre et Marie Curie-Paris 6, UMR5143, F-75005 Paris, France

F. Bassinot and N. Caillon
Laboratoire des Sciences du Climat et de l'Environnement, CFR, CNRS/CEA, Avenue de la Terrasse, F-91198 Gif-sur-Yvette, France

K. Charlier
Université Bordeaux I, DGO-UMR CNRS 5805 EPOC, Avenue des Facultés, F-33405 Talence, France

[1] High-resolution faunal and isotopic analyses of foraminifera were performed on core MD96-2073 (10°94′N, 52°62′E, 3142 m depth), located close to Socotra Island in the upwelling area of the Somali Basin (NW Indian Ocean). This work focuses on Marine Isotopic Stage 6.5 in order to reconstruct paleo-upwelling changes and their links with the Arabian Sea summer monsoon and the migration of the Intertropical Convergence Zone (ITCZ). Correspondence and cluster analyses of planktonic foraminiferal abundances, partly controlled by temperature and water mass productivity, together with an upwelling intensification index, show the occurrence of a strong upwelling between 176 and 165 ka. This upwelling intensification responds to a northward migration of the ITCZ. An isotopic depletion in the planktonic foraminifera $\delta^{18}O$ records occurring between 180 and 167 ka is interpreted as proof of a large salinity decrease in the surface waters, probably linked to a strong input of fresh rainfall waters induced by an intense monsoon activity. The lag between the onset of upwelling intensification and the strong monsoonal impact over the same area suggests a decoupling between both phenomena. The migration of the ITCZ is influenced by obliquity and precessional forcing, while the Arabian Sea summer monsoon precipitation depends only on precessional forcing.

Components: 9122 words, 6 figures.

Keywords: paleoclimatology; foraminifera; isotopes; Indian monsoon; ITCZ; sapropels; upwelling.

Index Terms: 4926 Paleoceanography: Glacial; 4934 Paleoceanography: Insolation forcing; 4964 Paleoceanography: Upwelling (4279).

Received 30 April 2006; **Revised** 22 September 2006; **Accepted** 18 October 2006; **Published** 29 December 2006.

Malaizé, B., C. Joly, M.-T. Vénec-Peyré, F. Bassinot, N. Caillon, and K. Charlier (2006), Phase lag between Intertropical Convergence Zone migration and subtropical monsoon onset over the northwestern Indian Ocean during Marine Isotopic Substage 6.5 (MIS 6.5), *Geochem. Geophys. Geosyst.*, *7*, Q12N08, doi:10.1029/2006GC001353.

Theme: Past Ocean Circulation
Guest Editors: Jean Lynch-Stielitz, Catherine Kissel, and Oliver Marchal

1. Introduction

[2] The strength of the meridional heat transfer between the equatorial region and the high latitudes plays a key role in climate change and influences meteorological phenomena such as the subtropical monsoons over Africa and India. The astronomical forcings which trigger these monsoons have been deciphered from detailed studies of geological records found in marine sediment cores collected from around northern parts of the African continent.

[3] Evidence of precessional forcing on these monsoons has previously been revealed in marine sedimentary records of the equatorial Atlantic Ocean [*Molfino and McIntyre*, 1990; *Schneider et al.*, 1997] and in estimations of monsoon-related continental rainfall over the African continent [*Partridge et al.*, 1997; *Gasse*, 2000]. Deposition of organic-rich layers called sapropels in the Mediterranean Sea has been associated with the strong discharge of fresh water, the origin of which could be ancient rivers [*Pachur and Kröpelin*, 1987], the partial summer melting of continental ice, notably from the Taurus mountains [*Kuzucuoglu et al.*, 1999], heavy discharge from the River Nile [*Rossignol-Strick*, 1985; *Fontugne et al.*, 1994], or enhanced precipitation either in the tropical belt or over the Mediterranean Basin [*Vergnaud Grazzini et al.*, 1986; *Kallel et al.*, 2000; *Bard et al.*, 2002]. These later hypotheses suggest a link between sapropel formation and monsoon. According to Rossignol-Strick, a sapropel is formed every time the monsoon index M, defined as the insolation gradient between the north tropic (23°N) and the equator, reaches a threshold value [*Rossignol-Strick*, 1983]. Increasing northern hemisphere summer insolation drives the monsoon index to cross this threshold and creates a sapropel layer in the Mediterranean Sea.

[4] In the equatorial Indian Ocean, monsoon imprints are mainly expressed by changes in wind stress, recorded for example by the eolian lithogenic fraction, and locally creating some coastal upwellings. For instance, stronger monsoonal summer winds intensify coastal upwelling near the coast of Arabia [*Ivanova et al.*, 2003; *Conan and Brummer*, 2000]. Previous works conducted on long marine records taken in the Arabian Sea have shown a precessional frequency in the occurrence of these upwellings [*Prell*, 1984; *Clemens and Prell*, 1990; *Rostek et al.*, 1997; *Ivanova et al.*, 2003]. Precession seems also to affect intermonsoon winds along the equatorial Indian Ocean [*Beaufort et al.*, 1997]. The latitudinal extension of the monsoonal upwelling area depends on the migration of the Intertropical Convergence Zone (i.e., ITCZ). The further north the ITCZ moves, the more upwelling occurs along the Arabian coast (Figure 1).

[5] In a recent study in the same area, a lag of several thousand years has been observed between periods of high primary productivity, driven by strong upwelling, and maximum summer insolation [*Ivanova et al.*, 2003]. A more precise study in the northwestern part of the Indian Ocean [*Clemens and Prell*, 1990] has analyzed the phasing between indicators of monsoon wind strength, such as the *Globigerina bulloides* upwelling record or lithogenic grain size, on the one hand, and indicators of source-area aridity/humidity such as mass accumulation rates (MAR), on the other. According to this study, MAR variations are in phase with global ice volume variations, but lead by 8 kyr the lithogenic grain size record. In an expanded study of the same area, the same authors showed that within the precession band, the peak amplitudes recorded in a summer-monsoon wind stack (obtained from five individual proxies all dependent on the strength of upwelling in the Owen ridge), occur 8 kyr after the maximum north hemisphere summer insolation and 3 kyr after ice-volume minima [*Clemens and Prell*, 2003]. These results suggest a time lag of several thousand years between the intensification of rainfall, which would depend upon the northern hemisphere insolation (according to *Rossignol-Strick*, 1983], and the increase of coastal upwelling inten-

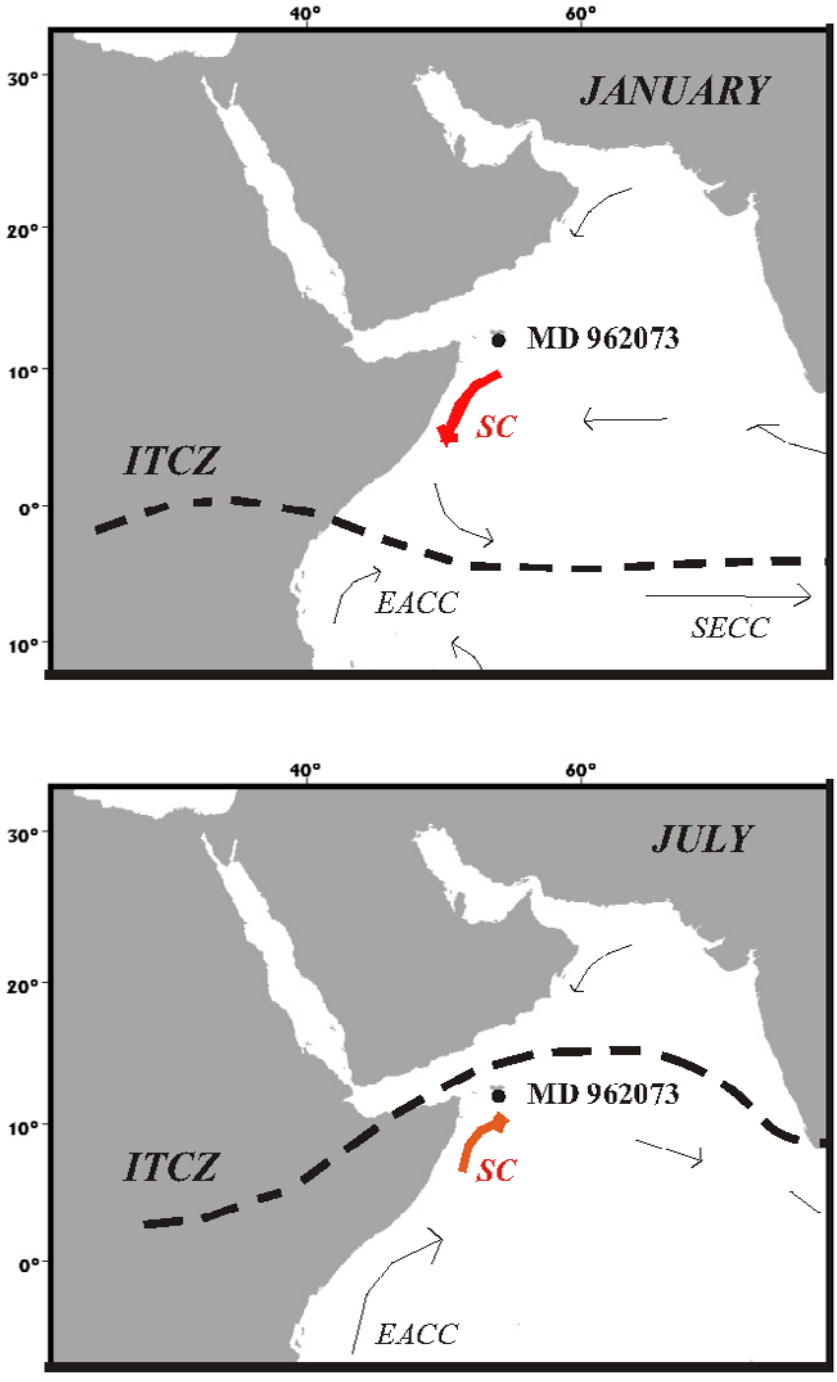

Figure 1. Location of core MD96 2073 and oceanic circulation in the western Indian Ocean. SC, Somali current; EACC, East Africa counter current; SECC, South Equatorial counter current.

sity in the N-W Indian Ocean, linked with the northward migration of the ITCZ. Recent modeling of the orbital signal in the Earth's climate by *Tuenter et al.* [2003] has shown that different forcings could be the answer to this time-lag and revealed the significant contribution of the obliquity signal in the African summer monsoon. Thus the strength of the African monsoon could depend more precisely on a combination of precession and obliquity. *Tuenter et al.* [2003] challenged the "data community" to find paleoclimatic records in which both obliquity and precessional forcings

could be found in order to test the sensitivity of tropical climate dynamics to these two astronomical forcing factors. The presence of obliquity-related oscillations has already been observed in Plio-Pleistocene marine sequences of the Mediterranean Sea [*Lourens et al.*, 1996], and also in the northern Arabian Sea [*Clemens and Prell*, 2003]. According to this last study, the compiled summer-monsoon upwelling intensity stack shows a stronger variance in the obliquity band (26%) than in the precession band (18%), indicating the importance of obliquity in the monsoon phenomena.

[6] Two questions arise from these previous works. What is the phasing between the increase of monsoon precipitation and the latitudinal extent and intensity of upwelling in the NW Indian Ocean, and their forcings? What is the phasing between Arabian and Mediterranean paleoclimatic imprints of monsoon?

[7] In order to answer these questions, we have analyzed marine sediment core MD96-2073, collected in the Socotra basin (Figure 1). This area is influenced by the Indian summer monsoon and seasonal upwelling occurs when the ITCZ moves northward (Figure 1). We will focus on different upwelling tracers, as well as monsoon imprints during Marine Isotopic Stage (MIS) 6.5, as defined in the SPECMAP marine record [*Martinson et al.*, 1987]. We have chosen this interval of the penultimate glacial period because imprints of strong monsoons have been observed during this time period [*Rossignol-Strick*, 1985; *Kallel et al.*, 2000; *Bard et al.*, 2002; *Clemens and Prell*, 2003]. Indeed, a peculiar situation is observed for sapropel S6, deposited in the Mediterranean Sea at around 175 ka during MIS 6.5. Although estimations of global continental ice volume, deduced from sea level reconstruction curves [*Waelbroeck et al.*, 2002], propose decreased sea level and therefore global glacial conditions at that time, many studies tend to demonstrate more humid conditions around the Mediterranean Basin. The $\delta^{18}O$ isotopic records obtained on some speleothems of the Soreq cave in Israel [*Ayalon et al.*, 2002] and the Argentarola cave in Italy [*Bard et al.*, 2002] revealed a shift to more negative values during MIS 6.5. The authors interpreted this depletion as the indication of an increase in rainfall over the entire Mediterranean Basin, an event coinciding with a maximum value in the 65°N insolation curve. A specific General Circulation Model (GCM) test has been performed at the LMD (Laboratoire de Météorologie Dynamique, CNRS Paris) by *Masson et al.* [2000], which compared insolation during the Last Glacial Maximum with the insolation during the penultimate glacial period. It showed a 50 w/m^2 excess in substage 6.5, which is sufficient to explain a stronger atmospheric meridional transfer, and therefore stronger Indian and African monsoon precipitations in the tropics at times of glacial conditions [*Masson et al.*, 2000]. Results of another atmospheric GCM also predicted higher precipitations between 180 and 170 ka [*Bard et al.*, 2002].

2. Material and Methods

[8] Core MD96-2073 (10°94′N, 52°62′E; 3142 m) was retrieved in 1996 during the MD 104-Pegasom cruise on the R/V *Marion Dufresne* under the Socotra gyre. A downcore biogenic and geochemical analysis was carried out by *Jacot Des Combes et al.* [2005]. Variations in the upwelling intensity, estimated from an Upwelling Radiolarian Index (URI), revealed that maximum upwelling intensity occurred within MIS 3. Investigation of MIS 6 faced interpretation problems, due either to the dominance of non-siliceous organisms in the planktonic community or to an increased terrigeneous input. For the purpose of this study, we have extensively analyzed Marine Isotopic Stage 6, focusing on a faunal and isotopic analysis of foraminifera. Mean sampling resolution is 10 cm along the penultimate glacial period, with increased resolution (every 5 cm) over specific time intervals.

[9] For the isotopic analysis, planktonic foraminifera *Globigerina bulloides* and *Globigerinoides ruber* have been picked within the 250–315 μm size fraction, and cleaned with distilled water. These two planktonic species have been chosen because their environmental behavior and isotopic signature are well known, especially in this northwestern part of the Indian Ocean [*Bé and Tolderlund*, 1971; *Kroon*, 1991; *Cullen and Prell*, 1984; *Kroon and Ganssen*, 1989; *Curry et al.*, 1992]. A *Micromass Multiprep* autosampler was used to prepare each aliquot (8 to 10 specimens, representing a mean weight of 80 μg) with an individual acid attack for each sample. The extracted CO_2 gas was analyzed against the international NBS 19 standard. The benthic fauna underwent the same preparation as for the planktonic foraminifera. We selected *Cibicides wuellestorfi* since its $\delta^{18}O$ is calibrated to the *Uvigerina* reference species [*Shackleton and Opdyke*, 1973; *Duplessy et al.*, 1984]. In agreement with previous studies, we applied a +0.64 per mil

correction factor to the measured $\delta^{18}O$ values against NBS 19. All the analyses were undertaken at the Department of Geology and Oceanography at Bordeaux University, UMR 5805 EPOC, using an *Optima Micromass* mass spectrometer. Standard deviations of multiple replicate measurements of NBS19 standard are 0.035 and 0.048 per mil for $\delta^{13}C$ and $\delta^{18}O$ measurements, respectively.

[10] The abundance of planktonic foraminiferal species is based on counts performed on fraction aliquots greater than 150 micron size fraction (containing at least 300 specimens) from the same sediment samples used for isotopic measurements (i.e., across the 160–180 ka time interval). A factorial correspondence analysis (FCA) [*Benzecri et al.*, 1973] and a hierarchical classification were performed through a statistical analysis of these census data using the SPAD.N program [*Centre International de Statistique et d'Informatique Appliquées*, 1991]. AFC combines the advantages of R-mode and Q-mode factor analysis. This technique resulted in a statistical partition of sediment samples in homogeneous clusters, which assists in interpreting the paleoenvironmental significance of the faunal record [*Vénec-Peyré et al.*, 1995, 1997; *Vénec-Peyré and Caulet*, 2000].

[11] Trace element analyses were performed at LSCE for Mg/Ca paleothermometry. Samples of *G. ruber* and *G. bulloides* were picked in the size fraction of 250–315 μm. Samples were cleaned following the method described by *Barker et al.* [2003] to eliminate contamination from clays and organic matter. Magnesium and calcium analyses were performed on a Varian Vista Pro Inductively Coupled Plasma Optical Emission Spectrometer (ICP-OES) following the procedure developed by *de Villiers et al.* [2002]. Precision for measured Mg/Ca ratios determined from replicate runs of a standard solution of Mg/Ca = 5.23 mmol/mol is 0.5% (1σ, RSD). Precisions obtained on *G. ruber* and *G. bulloides* samples are 3.0% and 5.0% respectively (1σ, pooled RSD).

3. Results

3.1. Stratigraphy of Core MD96-2073

[12] For the first study of this core, *Jacot Des Combes et al.* [2005] used an oxygen isotopic record of the bulk sediment and compared it to the planktonic isotopic curve (*G. bulloides*) obtained from adjacent core, MD 85682 [*Ouahdi*, 1997] in order to obtain a preliminary age model. In addition, they used the first appearance of the radiolarian species *Buccinosphaera invaginata* in core MD 962073, dated at 170 ± 10 ka in the Central Indian Basin [*Johnson et al.*, 1989].

[13] In this paper, we improved this age model for the penultimate climatic cycle. We used the oxygen isotopic record of *C. wuellerstorfi*, which partly represents global sea level changes during this penultimate climatic cycle, and compared it with the benthic SPECMAP record [*Martinson et al.*, 1987], taken as a reference (Figure 2a). Six age control points have been chosen at the main $\delta^{18}O$ variations found in both records. A last pointer has been selected at depth of 1676 cm in the Indian core, corresponding to a standstill in the ^{18}O depletion trend during Termination II. This standstill suggests a slow down or even a pause in the sea level rise. Such an event has been observed in other marine benthic records [*Lototskaya and Ganssen*, 1999; *Shackleton et al.*, 2003; *Gouzy et al.*, 2004] and corresponds to the growth of coral reef terraces dated around 128 ka (U/Th dating technique) in the western Pacific Aladdin's cave [*Esat et al.*, 1999] and around 129 ka for Barbados terraces [*Gallup et al.*, 2002]. We attribute an age of 128.5 ka to this last pointer. Using the *Analyserie* program [*Paillard et al.*, 1996], we finally obtained the age model presented in Figure 2a by linearly interpolating ages between the selected control points.

[14] These two independent age models (this study and *Jacot Des Combes et al.* [2005]) show good agreement (correlating factor between the two curves is r = 0.96) (Figure 2b) leading to a confidence in our age-model with an uncertainty of about ±3 kyr. The mean accumulation rate is about 8 cm/kyr. The 10 cm sampling interval corresponds to a mean temporal resolution of 1250 years and the higher-resolution sampling (each 5 cm) to a time interval of approximately 625 years.

3.2. Planktonic Foraminiferal Assemblages

[15] The cluster analysis applied to the data set of the planktonic assemblages allows a statistical discrimination of the sediment samples into five separate clusters. This clustering takes into account the information extracted by the first ten factors of the correspondence analysis, which explain most (90%) of the data set variance. Figure 3 shows these clusters plotted on a bidimensional space

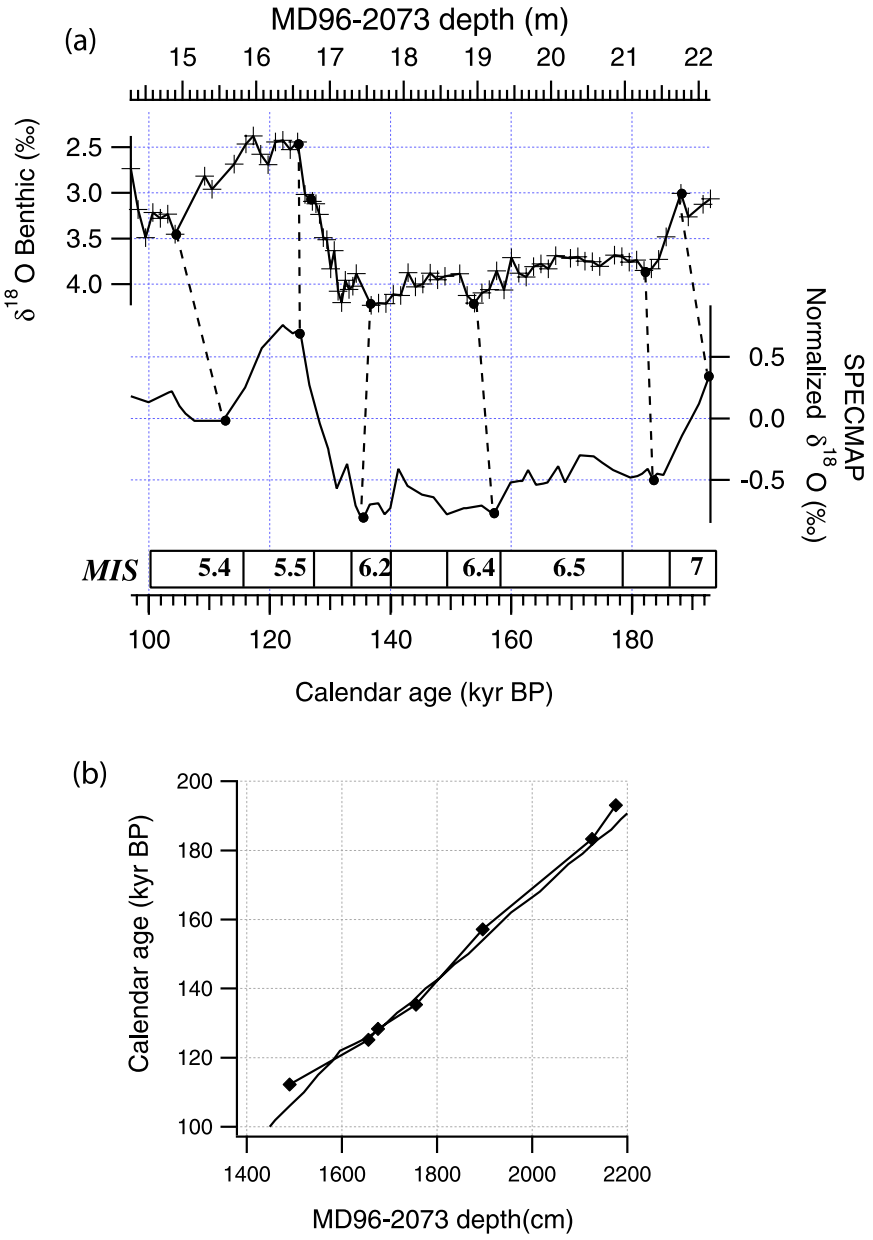

Figure 2. (a) (top) δ^{18}O record of *C. wuellerstorfi* benthic foraminiferal species of core MD 96 2073. (bottom) SPECMAP record [*Martinson et al.*, 1987] with most of the Marine Isotopic Stages (MIS) labeled. (b) Age scale obtained in this study (square marks) and by *Jacot Des Combes et al.* [2005].

defined by the first two axes (factorial plot $^1/_2$) which explain respectively 37.8% and 12% of the variance in the data set. For the sake of clarity, we will detail herein only clusters A and C, which cover the period studied in this paper. Other clusters will be analyzed in future work (in progress).

[16] The mean relative abundances of the main foraminiferal species or group of species which characterize these two clusters are also plotted in Figure 3. We have considered several categories according to the ecological requirements of species [*Bé and Tolderlund*, 1971; *Bé and Hutson*, 1977; *Cullen and Prell*, 1984; *Kroon*, 1991; *Sautter and Thunell*, 1991; *Anderson et al.*, 1992; *Thiede and Junger*, 1992]. A monospecific group is composed of *dextral Neogloboquadrina pachyderma* (Ehrenberg, 1861), a species which prefers temperate to cold waters and which is also well-known to

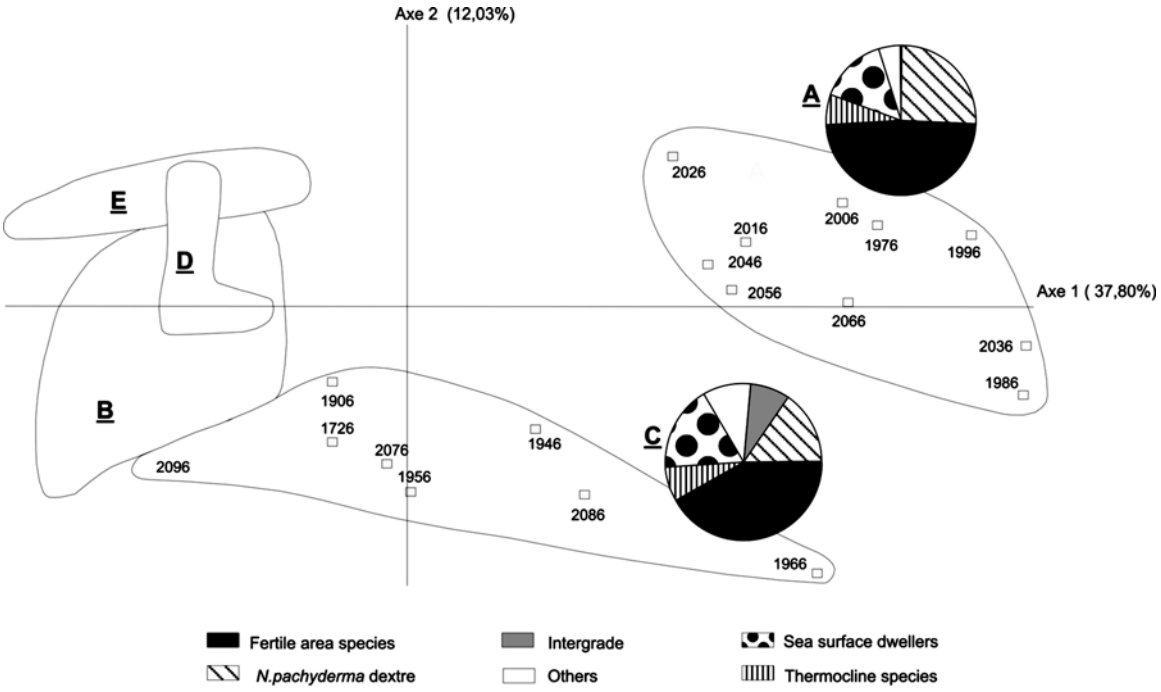

Figure 3. Distribution pattern of clusters based on samples collected between 15 and 22 meter depth in core MD96 2073 on the factorial plot $^{1}/_{2}$. The sample depth and the mean relative abundance of the main foraminiferal groups, presented as pie diagrams, are only plotted for clusters A and C (see text for details), which group only the samples settled during substage MIS 6.5 focused in this paper.

develop in tropical and subtropical upwelling areas. A second category includes several species known for their high abundance in nutrient-rich areas: *Globigerina bulloides* (d'Orbigny, 1826), *Globigerina falconensis* (Blow, 1959), *Globigerinita glutinata* (Egger, 1893) and *Neogloboquadrina dutertrei* (d'Orbigny, 1839). The third group includes species which live at or below the thermocline: *Globorotalia menardii* (Parker, Jones and Brady, 1865), *Globorotalia tumida* (Brady, 1877), *Pulleniatina obliquiloculata* (Parker and Jones, 1865) and *Globorotalia crassaformis* (Galloway and Wissler, 1927). The fourth group includes the sea surface dwellers: *Globigerinoides ruber* (d'Orbigny, 1839), *Globigerinoides sacculifer* (Brady, 1877) (including *G. trilobus*), *Globigerinoides conglobatus* (Brady, 1879) and *Globigerinella calida* (Parker, 1962), species that mainly live at low latitudes and are adapted to oligotrophic conditions. A further category groups the ''intergrades'' which represent morphological intergradation between the cold to temperate waters *N. pachyderma* and the species *N. dutertrei* which prefers warmer temperatures.

[17] Cluster A covers the upper right part of the factorial plot and includes 10 sediment samples deposited during MIS 6.5, from 2066 to 1966 cm. The foraminiferal assemblage is characterized by the following mean percentages: 48% of species known for their high abundance in fertile areas, 26% of dextral N. *pachyderma*, 15% of sea surface dwellers, and 7% of thermocline dwellers.

[18] Cluster C, spreading over the lower part of the factorial plot, is composed of all the sediment samples deposited just before (from 2076 to 2096 cm in the core) and after (from 1906 to 1966 cm) those which belong to cluster A. This cluster also includes the sediment sample selected at depth 1726 cm, deposited during MIS 6.2. The species which characterize fertile areas represent the most abundant group in this cluster, as in cluster A, with a mean value of about 42%; however, the mean percentage of dextral *N. pachyderma* (15%) is lower than in cluster A. The mean relative abundances of sea surface dwellers (18%), and of thermocline dwellers (7%) are close to the values observed in cluster A.

[19] Thus the species well-known to develop in temperate to cold and/or high nutrient level waters

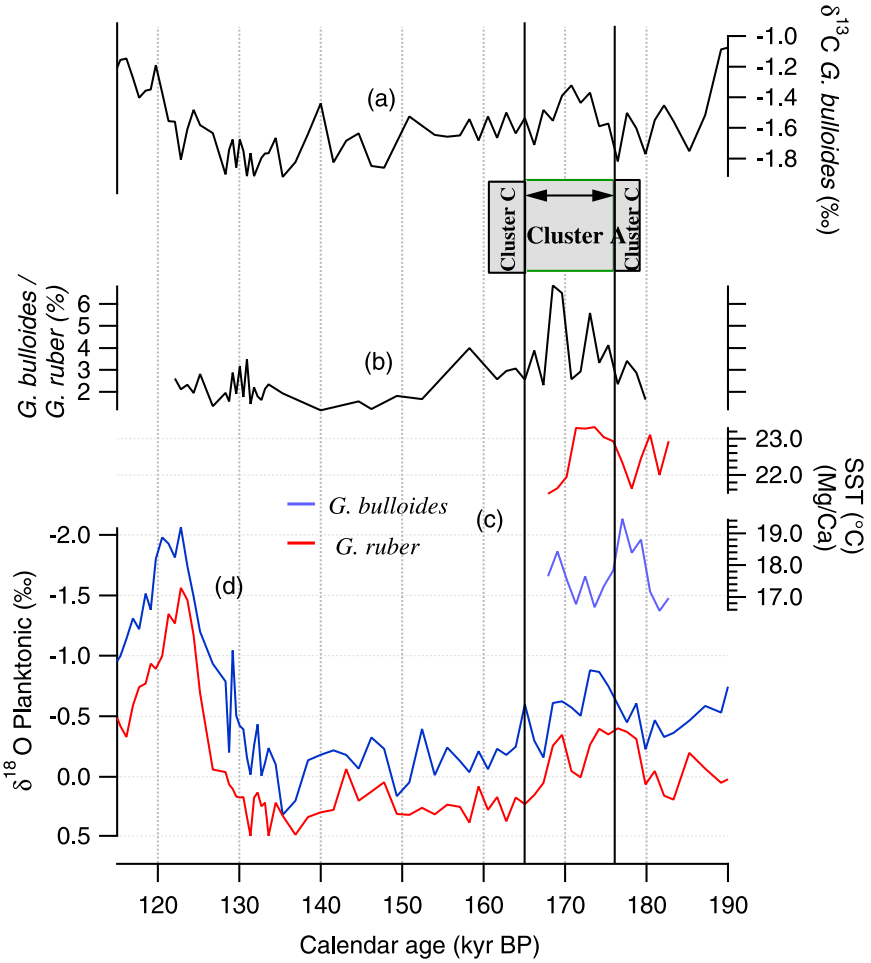

Figure 4. (a) δ^{13}C record of *G bulloides* planktonic foraminifera. (b) Abundance ratio *G. bulloides*/*G. ruber* as an upwelling strength indicator. (c) Sea Surface Temperature estimations, using Mg/Ca measurements (SST calibrated from *Anand et al.* [2003]): *G. bulloides*, blue line; *G. ruber*, red line. (d) δ^{18}O record of planktonic foraminifera: *G. bulloides*, blue line; *G. ruber*, red line.

make up 74% of the planktonic foraminiferal fauna in cluster A, whereas they account only for 57% in cluster C.

4. Discussion

4.1. Upwelling Biological and Isotopic Signatures

[20] We present in Figure 4 the δ^{18}O records of planktonic foraminiferal species *G. ruber* and *G. bulloides*. The spreading of clusters A and C as defined previously, is also shown.

[21] The time interval covered by cluster A starts at around 176 ka and ends at around 165 ka (within isotopic substage 6.5). It is characterized by the high abundance of the species known to proliferate in fertile areas (the strongest values observed along this penultimate glacial period), together with a relative abundance of relatively cold water species (dextral *N. pachyderma*). This faunal association could clearly be linked with an intensification of the Socotra upwelling, which brings nutrient-rich waters and strengthens sea surface productivity during substage 6.5. Sediments settling just before and after this particular episode correspond to cluster C, in which the decrease of dextral *N. pachyderma* and "fertile area" species suggests a decline in cold and productive surface waters.

[22] These observations are underscored by a downcore evolution of the upwelling intensification index proposed for this area by *Conan and Brummer* [2000]. These authors analyzed the faunal composition of sediment traps in the Socotra

upwelling region (10°45, 44N–51°56,50E), west of core MD96-2073. During the strengthening of the SW monsoon, they noticed a very important increase in the fluxes of *G. bulloides*, while the fluxes of *G. ruber* stayed roughly stable throughout the entire year. They suggested that the *G. bulloides*/*G. ruber* abundance ratio is linked to the strength of the upwelling. Applied to core MD96-2073, this index shows higher values (Figure 4) within the same time interval as the one defined for cluster A, and appears to confirm our hypothesis of a stronger upwelling in this area during MIS 6.5.

[23] In addition, measurements of Mg/Ca ratio on both planktonic foraminiferal species *G. ruber* and *G. bulloides* have been made to allow an estimation of past Sea Surface Temperature variations (SST), based on previous calibrations published for these species [*Anand et al.*, 2003]. Since *G. bulloides* mainly grow during the summer season, when the SW monsoon induces the Socotran upwelling, SST estimates extracted from this species are mainly representative of the upwelled waters. Our results show a 2°C drop at around 176 ka, suggesting the advection of cold waters (Figure 4). This confirms the intensification of the Socotran upwelling at this time, in good accordance with foraminiferal assemblages (occurrence of cluster A). Meanwhile, SST variations deduced from Mg/Ca measurements on *G. ruber* species show a surprising increase of about 1.6°C, indicating warmer sea surface conditions. This opposition between estimated SST variations can be explained by the seasonality of these species. As shown by *Curry et al.* [1992] and *Conan and Brummer* [2000], in the western part of the Indian Ocean, where upwellings are taking place, *G. bulloides* flux increases during the summer season; on the contrary, highest fluxes of *G. ruber* (much smaller in amplitude than *G. bulloides* flux) occur during both seasons, i.e., the summer season and the winter stratification season during which *G. bulloides* flux is highly reduced. According to *Curry et al.* [1992], this winter seasonal opposition does not exist in the less productive central and eastern parts of the Indian Ocean. A comparison of the two curves representing the SST estimates (Figure 4) allows a discrimination between two phases. Before 176 ka, the two curves show the same trends, whereas after 176 ka the observed anti-correlation seems to confirm the enhancement of the upwelling.

[24] Moreover, higher productivity related to a strong upwelling should lead to an enrichment in ^{13}C of the dissolved carbon in the surface waters, which should be recorded in surface dweller's tests. Such an increase in the *G. bulloides* $\delta^{13}C$ record has been observed under high productivity conditions in the equatorial Atlantic (Congo Basin) [*Schneider et al.*, 1994] and some isotopic measurements made on living species of *G. bulloides* in the coastal upwelling areas of the Arabian Sea have shown an enrichment in $\delta^{13}C$ values [*Kroon and Ganssen*, 1989]. The carbon isotopic record of the planktonic foraminifera *G. bulloides* in core MD96-2073 shows indeed higher values of $\delta^{13}C$ (0.4 per mil compared to a 0.8 permil glacial-interglacial shift), within the time period 176 ka to 166 ka, which is also characterized by lower *G. bulloides* SST and correspond to cluster A (stronger upwelling) (Figure 4).

[25] A more accurate interpretation of our results reveals the exact timing of the onset of the stronger upwelling. According to the foraminiferal cluster analysis the increase of the upwelling seems to start at 176 ka at the boundary between cluster C and A, when the species well-known to develop in temperate to cold and/or high nutrient level waters increase from 57% to 74%. However, the *G. bulloides*/*G. ruber* ratio, together with the $\delta^{13}C$ record from *G. bulloides*, shows some small variations prior to 176 ka. These small wiggles could suggest some earlier start in the strengthening of the upwelling, maybe at around 180 ka. Nevertheless, two arguments lead us to locate the increased upwelling intensity at 176 ka rather than 180 ka. First, the cluster analysis rests upon a statistical observation of all species present in the samples, while the *G. bulloides*/*G. ruber* index deals only with two species, which are less representative as they form only a part of the assemblages (26% for *G. bulloides* within cluster A, and 7% for the *G. ruber*). Furthermore, as pointed out by *Kroon and Ganssen*, both of these species could represent different phases in the upwelling system [*Kroon and Ganssen*, 1989] and their relation to upwelling dynamics may have changed over time which makes the *G. bulloides*/*G. ruber* index more questionable. The second argument is even more convincing. As the upwelled waters are characterized by cold temperatures, the 2°C drop in SSTs deduced from Mg/Ca measurements on *G. bulloides*, starts after 177 ka. Between 180 and 177 ka, the G. *bulloides* SST increased by 2°C, which would not be coherent with a strengthened upwelling at that time.

[26] To conclude, the concordant downcore evolution of the faunal and geochemical proxies studied in core MD96-2073 seems to reflect a strengthening of the upwelling activity during isotopic substage 6.5, starting at around 176 ka.

4.2. Monsoon-Related Precipitations Over the Region

[27] Today, strong monsoons are responsible for intense precipitation in this part of the Indian Ocean. In the past, as mentioned in the introduction of this paper, evidence of strong monsoon-related precipitations during isotopic substage 6.5 has been observed in paleo-records [*Rossignol-Strick*, 1983; *Cayre et al.*, 1999; *Bard et al.*, 2002] as well as inferred by GCM results [*Masson et al.*, 2000; *Bard et al.*, 2002]. Therefore it is possible that evidence of strong precipitation could be observed in sections of the core MD96-2073 covering this specific time interval.

[28] The $\delta^{18}O$ records of both planktonic foraminifera show depletions during isotopic substage 6.5, starting at around 180 ka (Figure 4). Three hypotheses could be proposed to explain such changes in the oxygen isotopic ratios: (1) Global dilution in the world ocean due to glacial/interglacial melting of the continental ice caps, (2) SST changes, or (3) Sea Surface Salinity (SSS) changes.

[29] To evaluate the component of the planktonic $\delta^{18}O$ signal linked to global continental ice volume changes, one needs to look at the corresponding benthic isotopic record (Figure 2). Changes in benthic $\delta^{18}O$ values are of about 0.25 per mil, which represent less than 15% of the total glacial/interglacial $\delta^{18}O$ change in the benthic curve (1.7 per mil). The planktonic $\delta^{18}O$ variations recorded during substage 6.5 are approximately 0.7 per mil. The amount of variation in the benthic $\delta^{18}O$ record is insufficient to explain the whole isotopic depletion signal record in the planktonic curve, and the difference is probably linked to other surface parameter changes.

[30] To quantify the component of the planktonic $\delta^{18}O$ decrease due to temperature changes over the whole year (and not only specific to the upwelling season), we focused on the estimation of past SST variations deduced from Mg/Ca ratio in *G. ruber* foraminifera (Figure 4). A first SST decrease is recorded in the first part of the signal, from 180 to 178 ka. Then, as mentioned previously, warmer temperatures characterize surface waters during MIS 6.5, with a strong increase from 21,5°C to more than 23°C between 178 and 174 ka, and a strong decrease of about the same amplitude between 171 and 168 ka.

[31] According to the isotopic paleotemperature equation established by pioneer studies [*Epstein et al.*, 1953; *Shackleton*, 1974], the oxygen fractionation between foraminiferal calcite and the surrounding water increases by about 0.25 per mil for each degree the water is cooled. If the amplitude of these high SST changes could explain lower values in the planktonic $\delta^{18}O$ curve from 178 ka to 174 ka, the records contradict one another for the previous 2 kyr. The depletion in the *G. ruber* $\delta^{18}O$ record clearly starts at around 180 ka, while the Mg/Ca SST record shows a coincident drop from 23°C to 21°C (Figure 4). During this time period, the planktonic isotopic signal cannot be directly driven by a SST change. To fully understand the planktonic isotopic signal, we must estimate SSS changes over the MIS 6.5.

[32] Sea Surface Salinity (SSS) changes have been calculated following the work of *Duplessy et al.* [1991] by removing the contribution of SST (estimated with Mg/Ca) and global sea level changes [*Waelbroeck et al.*, 2002] to the planktonic $\delta^{18}O$ record. The results show two clear freshening events of sea surface waters, a first starting at 180 ka and lasting until 174 ka, and a second one between 171 and 168 ka (Figure 5). The SSS uncertainties are dependent on uncertainties associated with the three components of the reconstruction, namely the $\delta^{18}O$ measurements of *G. ruber*, its Mg/Ca-based SST estimates and the global seawater $\delta^{18}O$ linked to sea level changes. The 3% uncertainty linked to SST estimates from *G. ruber* Mg/Ca measurements correspond to a 0.08 per mil uncertainty on a δ scale, and a 0.15 per mil uncertainty is tied to global seawater $\delta^{18}O$ changes due to sea level changes within MIS 6 [*Waelbroeck et al.*, 2002]. The final uncertainty for the SSS calculation is about 0.176 per mil on a δ scale, which corresponds to a 0.352 per mil on a salinity scale. We are aware that this uncertainty represents more than one third of the maximum shift (1 per mil) of our SSS record. However, the two most drastic SSS events on which the discussion is based have an amplitude which exceeds our estimated error bar and therefore appear to be strongly supported by our data. Two hypotheses can be proposed to explain the origin of these low salinity waters.

[33] First, the peculiar setting of the western Arabian Sea, as an evaporative basin, leads to a strong

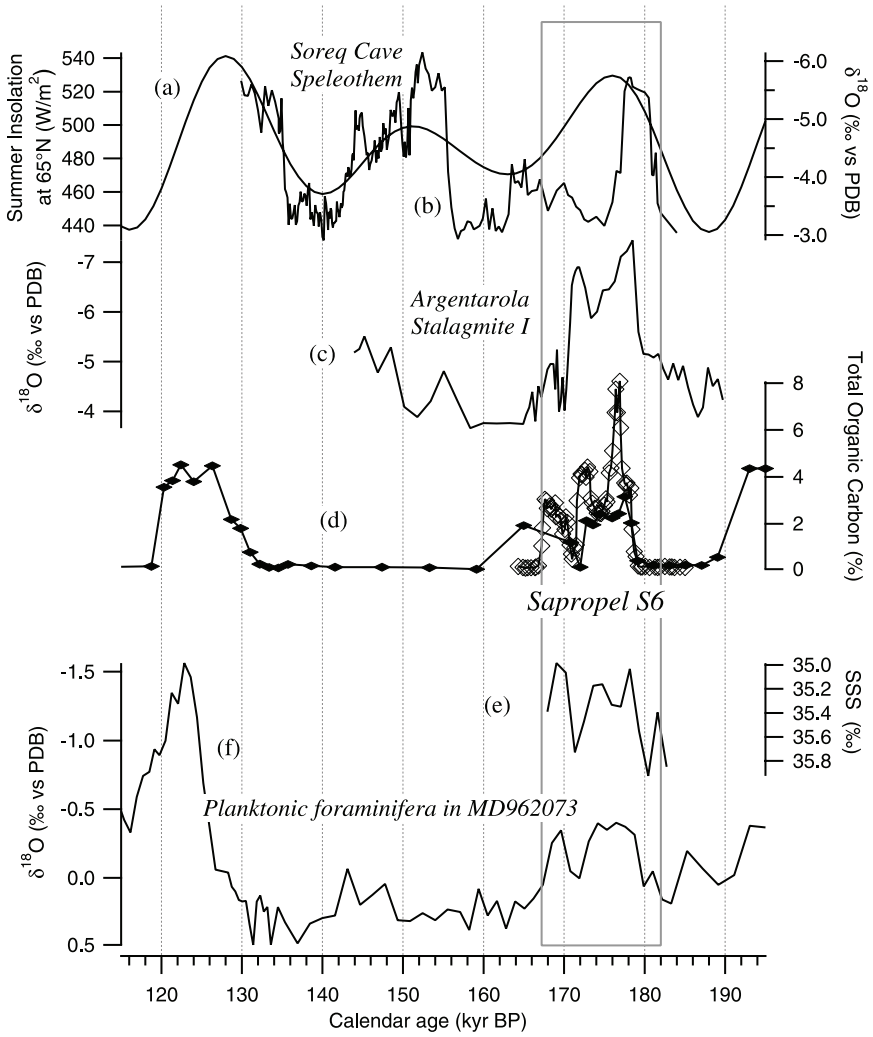

Figure 5. (a) Summer insolation at 65°N [*Berger*, 1978]. (b) δ^{18}O record of Soreq Cave speleothem [*Ayalon et al.*, 2002]. (c) δ^{18}O record of Argentarola stalagmite [*Bard et al.*, 2002]. (d) TOC variations (in wt%) in two well-studied marine cores: black diamonds are for MD84641 [*Kallel et al.*, 2000], and open diamonds are for KC19C [*Bard et al.*, 2002]. (e) Sea Surface Salinity reconstructions (see text for details). (f) δ^{18}O record of planktonic foraminifera: *G. bulloides*.

halocline, with high salinity at the surface, and lower salinity for intermediate waters. At the beginning of an upwelling intensification, the first upwelled waters would decrease the sea surface salinity. However, in the studied record, the first drastic SSS change occurs at 180 ka, 4 kyr before the beginning of the upwelling, as shown by foraminifer assemblages and G. *bulloides* SST. Therefore we believe that this first salinity signal is not a signature of upwelled waters.

[34] The second hypothesis, that we favor, deals with a direct link with strong precipitation events, when higher rainfall lead to fresh water discharges into the Socotra Basin. Monsoon precipitation δ^{18}O values have been estimated as between −6 to −12 per mil through isotopic measurements on African paleo-lake carbonates [*Gasse*, 2000]. As long as precipitation is expected to be depleted in ^{18}O with regards to the mean isotopic values of the ocean, low δ^{18}O values recorded in planktonic foraminifera shells could be a signature of a fresh water input to the ocean surface and likely linked to more intense rainfall. Indeed, these shifts to reduced δ^{18}O values have been observed in *G. ruber* foraminiferal species in Mediterranean Sea sediment cores during monsoon seasons [*Rohling et al.*, 2002].

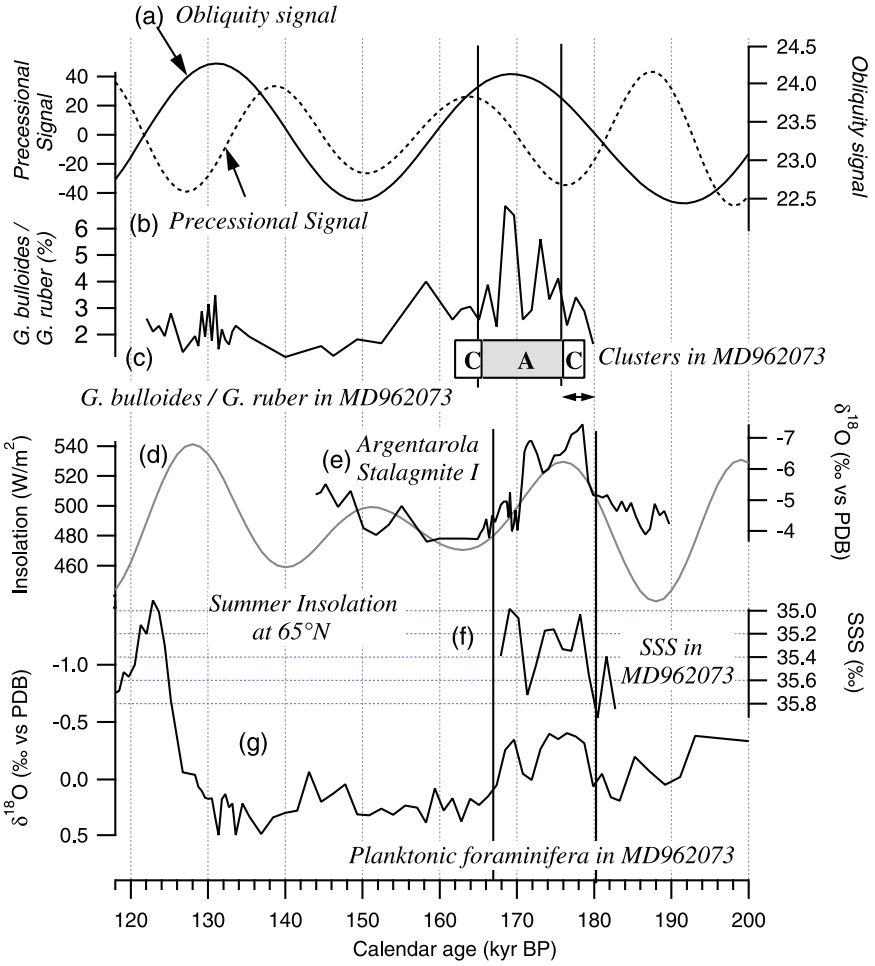

Figure 6. (a) Solid line: Obliquity signal [*Berger*, 1978]. (b) Dotted line: precessional signal [*Berger*, 1978]. (c) Abundance ratio *G. bulloides*/*G. ruber* in MD96 2073. (d) Summer insolation signal at 65°N [*Berger*, 1978]. (e) δ^{18}O record of Argentarola stalagmite [*Bard et al.*, 2002]. (f) Sea Surface salinity reconstructions. (g) δ^{18}O record of planktonic foraminifera: *G. bulloides*.

[35] According to *Jung et al.* [2001], during the period of strong monsoon in early Holocene, the Red Sea region could have been affected by strong precipitations, that may have lowered the Red Seawaters (RSW) advected to the Arabian Sea. However, we cannot suspect a possible influence of the Red Sea to explain these freshening events in the Socotra Basin during global low sea level conditions, because the very shallow sill depth of the Strait of Bab el Mandeb makes it unlikely that large exchanges existed between the Red Sea and the Arabian Sea at that time. We argue for a more general precipitation pattern, covering not only the Arabian region, but also higher latitudes, possibly reaching some part of the Mediterranean Sea. This hypothesis seems to be robust when compared with other paleoclimatic results obtained on speleothems of the Soreq Cave in Israel [*Ayalon et al.*, 2002], and of the Argentarola Cave in Italy [*Bard et al.*, 2002]. The δ^{18}O isotopic records obtained from these speleothems also revealed a shift to more negative values between 182 and 175 ka (^{230}Th/U ages) for the Soreq Cave and between 180 and 170 for the Italian Cave (Figure 5). In addition, the double-peaked shape detected in our SSS record is also seen in sapropel S6 recorded in the eastern part of the Mediterranean Sea, as shown by the TOC records retrieved from cores KC19c and MD84641 [*Bard et al.*, 2002]. This double peak is believed to show real precipitation fluctuations [*Bard et al.*, 2002]. These elements lead us to think that the same dramatic increase of rainfall over Middle East region during substage 6.5 had consequences not only over the entire Mediterranean region, but also over the northwestern part of the Indian Ocean.

[36] In Core MD96-2073, as all the proxies were studied in the same samples, there is no mismatch problem when considering the leads and lags between the observed events. This makes it possible to study in detail the sequence of climatic events. A clear lag is observed between the low salinity signal, as detected through planktonic $\delta^{18}O$ records, and the intensification of the upwelling described through three different proxies (Figure 6). The signature of enhanced precipitation starts no less than 4 kyr before the onset of strong upwelling. Providing that monsoon-precipitations are directly linked to northern hemisphere increase in insolation [*Rossignol-Strick*, 1983], the lag between precipitation and upwelling intensity appears to be coherent with the lag observed by *Ivanova et al.* [2003] between maximum northern summer insolation and the intensification of the Oman upwelling. It is also coherent with the lag observed by *Clemens and Prell* [2003] between the maximum northern hemisphere summer insolation and the strongest record of their summer-monsoon wind stack, deduced from five individual proxies linked to the upwelling intensity. This suggests that these the rainfall pattern (under control of maximum summer insolation) and upwelling intensity, that are a priori linked to the same meteorological phenomenon (the Indian monsoon), were somehow decoupled through time and show a complex response to insolation forcing and/or climatic boundary conditions.

[37] Today, in the Socotra Basin, stronger upwelling occurs during the summer when the ITCZ is moving northward. Thus the record of strong upwelling conditions revealed by our data set starting after 176 ka suggests a northward migration of the mean ITCZ position at this time. Recent modeling work proposed a trigger on the latitudinal position of the ITCZ [*Tuenter et al.*, 2003] using a combination of precession and obliquity signals: a northward movement of the ITCZ appears to take place when obliquity reaches a high value and precession is very weak (negative values). In the studied record, the upwelling started to strengthen at 176 ka, just when precession is at its minimum value and while obliquity is in an increasing phase (Figure 6). Before 176 ka, even if precession is still weak, obliquity has not yet reached its highest value, thus preventing the ITCZ from moving northward and the upwelling from developing near the coast of Socotra.

[38] Similar orbital parameter conditions favoring a northward migration of the ITCZ (i.e., low precession together with high obliquity) are also observed between 134 and 122 ka. Other evidence for a northward penetration of the ITCZ over North Africa during the Eemian (at around 122 ka) have been put forth through *G. rubber* $\delta^{18}O$ isotopic records in the Mediterranean Basin [*Rohling et al.*, 2002]. In core MD96-2073, the response of upwelling tracers (such as *G. bulloides*/*G. ruber* ratio) shows some variation, but with a lower amplitude than during MIS 6. This can be explained by different environmental settings of the Socotra basin due to the sea level rise and sea surface temperature rise during this termination II. In Core MD96-2073 the *G. bulloides*/*G. ruber* curve shows small variations just after the global sea level rise which occurred at 136 ka according to the benthic isotopic curve (Figure 2). As suggest by Jung et al., an outflow of Red Seawaters (RSW) might have had a strong influence into the Arabian Sea during interglacial period [*Jung et al.*, 2001]. A RSW outflow into the Socotra Basin could induce a warmer sea surface temperature and a higher stratification of water masses, disturbing the ecological requirements for *G. bulloides* (i.e., usually cold and tropical nutrient rich waters). But, as we have discussed previously, during full glacial conditions (within MIS 6.5), such conditions could not occur because of a lower sea level and a shallower sill depth of the Strait of Bab el Mandeb which control this outflow intensity.

[39] In contrast, the increase in precipitation at around 180 ka is more in phase with the summer insolation curve at 65°N. At 188 ka, when the 65°N insolation is at its minimum, continental ice caps in the northern hemisphere had reached their maximum geographical extent in midlatitudes. As mentioned by some authors, this situation should drive a more intense atmospheric circulation within the meridional region. If the atmospheric moisture was not trapped in the continental ice, we would expect an abrupt discharge of this residual moisture through heavy rainfall at the maximum 65°N insolation curve [*Tuenter et al.*, 2003]. All the rainfall events recorded in the eastern Mediterranean Sea, as well as in the Socotra Basin, started with the increase of the northern hemisphere insolation curve and reached their maximum at 176 ka, in phase with the maximum value of the 65°N insolation curve.

[40] Our results give more precision to the model results obtained by *Tuenter et al.* [2003]. They reveal a clear lag between the beginning of equatorial to midlatitude strong monsoon conditions

and the onset of upwelling in the northwestern Arabian Sea during MIS 6.5. This suggests a decoupling between the monsoon-discharge phenomena (depending mainly on northern hemisphere summer insolation) and the position of the ITCZ, which depends on the locally combined influence of remote (obliquity) and local (low latitude insolation responding to precession) astronomical forcing.

5. Conclusions

[41] The different paleoenvironmental evidences encoded within the paleoproxies investigated in this study provide new information on the conditions that prevailed over the northwestern Indian Ocean during Marine Isotopic Substage 6.5. Strong upwelling, revealed by faunal associations and directly related to strong southwesterly monsoon winds, started at 176 ka. A depletion in the planktonic $\delta^{18}O$ record, interpreted as a signal of lower sea surface salinity due to stronger precipitation, is observed 4 kyr before, in phase with several other geological records of stronger rainfall around the Mediterranean Basin.

[42] Following the hypothesis that the increase of precipitation at middle to low latitudes is due to the onset of a strong monsoon rainfall between 180 ka and 170 ka, and that upwelling strength is bound to the latitudinal position of the ITCZ, the lag between paleoproxy variations observed in this study appears to indicate a decoupling at the orbital timescale between the two meteorological phenomena, linked to different response to astronomical forcing. If the monsoon-related precipitation is linked to northern hemisphere summer insolation gradient between 23°N and the equator [*Rossignol-Strick*, 1983] the strength of Socotra Basin upwelling could respond to a combination of remote and local forcing (i.e., precession together with obliquity).

[43] The peculiar climatic conditions prevailing during glacial isotopic substage 6.5 still have some secrets to be revealed. For example, did these intense atmospheric phenomena have an impact on the western equatorial coast of the African margin in the Atlantic Ocean, and what was the position of the ITCZ in this area at that time? [*Schneider et al.*, 1997]. The high-resolution study of marine records seems to be one way to constrain the lead/lag problem between environmental responses and to understand better the forcing factors involved in the equatorial area. To assess if the phase-lag observed in this study during MIS 6.5 can be generalized for other orbital configurations, longer records have to be analyzed.

Acknowledgments

[44] Special thanks to Marie-France Loutre, Martine Paterne, Jacques Giraudeau, Maria Sanchez-Goni, Frederique Eynaud, Philippe Martinez, Xavier Crosta, and William Fletcher for help and stimulating discussions, and also to Olivier Ther for the preparation of the samples. The authors would like to thank Edouard Bard for providing the Argentarola stalagmite data and Avner Ayalon for providing those of Soreq cave. The authors would also like to thank Eva Moreno for her help in the sampling of the core at the core repository of Département Histoire de la Terre, Muséum National d'Histoire Naturelle (MNHN), Paris. We would like to thank the anonymous reviewers for adding some new insights in the discussion, improving the quality of the paper. We acknowledge R. Baudoin from the Centre Statistique of the MNHN for his assistance in the statistical analysis. The sediment core has been collected thanks to the staff of the research vessel *Marion Dufresne*, supported by the French agencies Ministère de l'Education Nationale de la Recherche et de la Technologie (MENRT), Centre National de la Recherche Scientifique (CNRS), and Institut Paul Emile Victor (IPEV). The scientific lead of the PEGASOM scientific cruise was J. P. Caulet. This work is a contribution to the IMAGES program. Financial support has been provided through ECLIPSE program. This paper is contribution 1565 of UMR 5805 EPOC, Bordeaux1 University.

References

Anand, P., H. Elderfield, and M. H. Conte (2003), Calibration of Mg/Ca thermometry in planktonic foraminifera from a sediment trap time series, *Paleoceanography*, *18*(2), 1050, doi:10.1029/2002PA000846.

Anderson, D. M., J. C. Brock, and W. L. Prell (1992), Physical upwelling processes, upper ocean environment and the sediment record of the southwest monsoon, in *Upwelling Systems: Evolution Since the Early Miocene*, edited by C. P. Summerhayes et al., *Geol. Soc. Spec. Publ.*, *64*, 121–129.

Ayalon, A., M. Bar-Matthews, and A. Kaufman (2002), Climatic conditions during marine oxygen isotope stage 6 in the eastern Mediterranean region from the isotopic composition of speleothems of Soreq Cave, Israel, *Geology*, *30*(4), 303–306.

Bard, E., G. Delaygue, F. Rostek, F. Antonioli, S. Silenzi, and D. P. Schrag (2002), Hydrological conditions over the western Mediterranean basin during the deposition of the cold Sapropel 6 (ca. 175 kyr BP), *Earth Planet. Sci. Lett.*, *202*, 481–494.

Barker, S., M. Greaves, and H. Elderfield (2003), A study of cleaning procedures used for foraminiferal Mg/Ca paleothermometry, *Geochem. Geophys. Geosyst.*, *4*(9), 8407, doi:10.1029/2003GC000559.

Bé, A. W. H., and W. H. Hutson (1977), Ecology of planktonic foraminifera and biogeographic patterns of life and fossil assemblages in the Indian Ocean, *Micropaleontology*, *23*(4), 369–414.

Bé, A. W. H., and D. S. Tolderlund (1971), Distribution and ecology of living planktonic foraminifera in surface waters of the Atlantic and Indian Oceans, in *Micropaleontology of Oceans*, edited by B. M. Funnell and W. R. Riedel, pp. 105–149, Cambridge Univ. Press, New York.

Beaufort, L., Y. Lancelot, P. Camberlin, O. Cayre, E. Vincent, F. Bassinot, and L. Labeyrie (1997), Insolation cycles as a major control of Equatorial Indian Ocean Primary Production, *Science*, *278*, 1451–1454.

Benzecri, F., et al. (Eds.) (1973), *L'Analyse des Données, II, L'Analyse des Correspondances*, 619 pp., Dunod, Paris.

Berger, A. (1978), Long-term variations of daily insolation and Quaternary climate change, *J. Atmos. Sci.*, *35*, 2362–2367.

Cayre, O., L. Beaufort, and E. Vincent (1999), Paleoproductivity in the Equatorial Indian Ocean for the last 260,000 yr: A transfer function based on planktonic foraminifera, *Quat. Sci. Rev.*, *18*, 839–857.

Centre International de Statistique et d'Informatique Appliquées (CISIA) (1991), *SPAD.N Intégré*, 137 pp., Saint Mandé, France.

Clemens, S. C., and W. L. Prell (1990), Late Pleistocene variability of Arabian sea summer monsoon winds and continental aridity: Eolian records from the lithogenic component of deep-sea sediments, *Paleoceanography*, *5*(2), 109–145.

Clemens, S. C., and W. L. Prell (2003), A 350,000 year summer-monsoon multi-proxy stack from the Owen Ridge, Northern Arabian Sea, *Mar. Geol.*, *201*, 35–51.

Conan, S. M.-H., and G.-J. A. Brummer (2000), Fluxes of planktic foraminifera in response to monsoonal upwelling on the Somalia Basin margin, *Deep Sea Res., Part II*, *47*, 2207–2227.

Cullen, J. L., and W. L. Prell (1984), Planktonic foraminifera of the northern Indian Ocean: Distribution and preservation in surface sediments, *Mar. Micropaleontol.*, *9*, 1–52.

Curry, W. B., D. R. Ostermann, M. V. S. Guptha, and V. Ittekkot (1992), Foraminiferal production and monsoonal upwelling in the Arabian Sea: Evidence from sediment traps, in *Upwelling Systems: Evolution Since the Early Miocene*, edited by C. P. Summerhayes et al., *Geol. Soc. Spec. Publ.*, *64*, 93–106.

de Villiers, S., M. Greaves, and H. Elderfield (2002), An intensity ratio calibration method for the accurate determination of Mg/Ca and Sr/Ca of marine carbonates by ICP-AES, *Geochem. Geophys. Geosyst.*, *3*(1), 1001, doi:10.1029/2001GC000169.

Duplessy, J.-C., N. J. Shackleton, R. K. Matthews, W. Prell, W. F. Ruddiman, M. Caralp, and C. H. Hendy (1984), ^{13}C record of benthic foraminifera in the last interglacial ocean: Implications for the carbon cycle and the global deep water circulation, *Quat. Res.*, *21*, 225–243.

Duplessy, J.-C., L. Labeyrie, A. Juillet-Leclerc, F. Maitre, J. Duprat, and M. Sarnthein (1991), Surface salinity reconstruction of the North Atlantic Ocean during the last glacial maximum, *Oceanol. Acta*, *14*, 311–324.

Epstein, S., R. Buchsbaum, H. A. Lowenstam, and H. C. Urey (1953), Revised carbonate-water isotopic temperature scale, *Geol. Soc. Am. Bull.*, *64*, 1315–1325.

Esat, T. M., M. T. McCulloch, J. Chappell, B. Pillans, and A. Omura (1999), Rapid fluctuations in sea level recorded at Huon peninsula during the penultimate deglaciation, *Science*, *283*, 197–201.

Fontugne, M., M. Arnold, L. Labeyrie, M. Paterne, S. E. Calvert, and J.-C. Duplessy (1994) Paleoenvironment, sapropel chronology and Nile river discharge during the last 20 000 years as indicated by deep-sea sediment records in the Eastern Mediterranean, in *Late Quaternary Chronology and Paleoclimates of the Eastern Mediterranean*, edited by O. Bar-Yosef and R. S. Kra, pp. 57–88, Radiocarbon, Tucson, Ariz.

Gallup, C. D., H. Cheng, F. W. Taylor, and R. L. Edwards (2002), Direct determination of timing of sea level change during Termination II, *Science*, *295*, 310–313.

Gasse, F. (2000), Hydrological changes in the African tropics since the Last Glacial Maximum, *Quat. Sci. Rev.*, *19*, 189–211.

Gouzy, A., B. Malaizé, C. Pujol, and K. Charlier (2004), Climatic "pause" during Termination II identified in shallow and intermediate waters off the Iberian margin, *Quat. Sci. Rev.*, *23*, 1523–1528.

Ivanova, E., R. Schiebel, A. D. Singh, G. Schmiedl, H.-S. Niebler, and C. Hemleben (2003), Primary production in the Arabian Sea during the last 135 000 years, *Palaeogeogr. Palaeoclimatol. Palaeoecol.*, *197*, 61–82.

Jacot Des Combes, H., J.-P. Caulet, and N. Tribovillard (2005), Monitoring the variations of the Socotra upwelling system during the last 250 kyr: A biogenic and geochemical approach, *Palaeogeogr. Palaeoclimatol. Palaeoecol.*, *223*, 243–259.

Johnson, D. A., D. A. Schneider, C. A. Nigrini, J. P. Caulet, and D. V. Kent (1989), Pliocene-Pleistocene radiolarian events and magnetostratigraphic calibrations for the tropical Indian Ocean, *Mar. Micropaleontol.*, *14*, 33–66.

Jung, S. J. A., G. M. Ganssen, and G. R. Davies (2001), Multidecadal variations in the early Holocene outflow of Red Sea Water into the Arabian Sea, *Paleoceanography*, *16*(6), 658–668.

Kallel, N., J.-C. Duplessy, L. Labeyrie, M. Fontugne, M. Paterne, and M. Montacer (2000), Mediterranean pluvial periods and sapropel formation over the last 200 000 years, *Palaeogeogr. Palaeoclimatol. Palaeoecol.*, *157*, 45–58.

Kroon, D. (1991), Distribution of extant planktonic foraminiferal assemblages in Red Sea and northern Indian Ocean surface waters, *Rev. Esp. de Micropaleontol.*, *23*(1), 37–74.

Kroon, D., and G. Ganssen (1989), Northern Indian Ocean upwelling cells and the stable isotope composition of living planktonic foraminifers, *Deep Sea Res., Part A*, *36*(6), 1219–1236.

Kuzucuoglu, C., J. Bertaux, S. Black, M. Denèfle, M. Fontugne, M. Karabiyikoglu, K. Kashima, N. Limondin-Lozouet, D. Mouralis, and D. Orth (1999), Reconstruction of climatic changes during the upper Pleistocene, based on sediment records from the Konya basin (Central Anatolya, Turkey), *Geol. J.*, *34*, 175–198.

Lototskaya, A., and G. M. Ganssen (1999), The structure of Termination II (penultimate deglaciation and Eemian) in the North Atlantic, *Quat. Sci. Rev.*, *18*, 1641–1654.

Lourens, L. J., A. Antonarakou, F. J. Hilgen, A. A. M. Van Hoof, C. Vergnaud-Grazzini, and W. J. Zachariasse (1996), Evaluation of the Plio-Pleistocene astronomical timescale, *Paleoceanography*, *11*(4), 391–413.

Martinson, D., N. Pisias, J. Hays, J. Imbrie, T. Moore, and N. Shackleton (1987), Age dating and the orbital theory of the ice ages: Development of a high-resolution 0 to 300,000–year chronostratigraphy, *Quat. Res.*, *27*, 1–29.

Masson, M., P. Braconnot, J. Jouzel, N. de Noblet, R. Cheddadi, and O. Marchal (2000), Simulation of intense monsoons under glacial conditions, *Geophys. Res. Lett.*, *27*, 1747–1750.

Molfino, B., and A. McIntyre (1990), Precessional forcing of the nutricline dynamics in the Equatorial Atlantic, *Science*, *249*, 766–769.

Ouahdi, R. (1997), Variations de la productivité au nord-ouest de l'océan Indien lors des derniers 70 000 ans dans l'upwel-

ling de Socotra et de Somalie: Enregistrements géochimiques, *Bull. Soc. Geol. Fr.*, *168*, 93–107.

Pachur, H. J., and S. Kröpelin (1987), Wadi Howar: Paleoclimatic evidence from an extinct river system in the South-Eastern Sahara, *Science*, *237*, 289–300.

Paillard, D., L. Labeyrie, and P. Yiou (1996), Macintosh program makes time-series analysis easy, *Eos Trans. AGU*, *77*(39), 379.

Partridge, T. C., P. B. Demenocal, S. A. Lorentz, M. J. Paiker, and J. C. Vogel (1997), Orbital forcing of climate over South Africa: A 200,000–year rainfall record from the pretoria saltpan, *Quat. Sci. Rev.*, *16*, 1125–1133.

Prell, W. L. (1984), Monsoonal climate of the Arabian Sea during the late Quaternary: A response to changing solar radiation, in *Milankovitch and Climate*, Part 1, edited by A. L. Berger et al., pp. 349–366, Springer, New York.

Rohling, E. J., T. R. Cane, S. Cooke, M. Sprovieri, I. Bouloubassi, K. C. Emeis, R. Schiebel, D. Kroon, F. J. Jorissen, A. Lorre, and A. E. S. Kemp (2002), African monsoon variability during the previous interglacial maximum, *Earth Planet. Sci. Lett.*, *202*, 61–75.

Rossignol-Strick, M. (1983), African monsoons, an immediate climate response to orbital insolation, *Nature*, *304*, 46–49.

Rossignol-Strick, M. (1985), Mediterranean Quaternary sapropels, an immediate response of the African monsoon to variation of insolation, *Palaeogeogr. Palaeoclimatol. Palaeoecol.*, *49*, 237–263.

Rostek, F., E. Bard, L. Beaufort, C. Sonzogni, and G. Ganssen (1997), Sea surface temperature and productivity records for the past 240 kyr in the Arabian Sea, *Deep Sea Res., Part II*, *44*, 1461–1480.

Sautter, L. R., and R. C. Thunell (1991), Planktonic foraminiferal response to upwelling and seasonal hydrographic conditions: Sediment trap results from San Pedro Basin, Southern California Bight, *J. Foraminiferal Res.*, *21*(4), 347–363.

Schneider, R. R., P. J. Müller, and G. Wefer (1994), Late Quaternary paleoproductivity changes off the Congo deduced from stable carbon isotopes of planktonic foraminifera, *Palaeogeogr. Palaeoclimatol. Palaeoecol.*, *110*, 255–274.

Schneider, R., B. Price, P. J. Müller, D. Kroon, and I. Alexander (1997), Monsoon related variations in Zaire (Congo) sediment load and influence of fluvial silicate supply on marine productivity in the east equatorial Atlantique during the last 200,000 years, *Paleoceanography*, *12*(3), 463–481.

Shackleton, N. J. (1974), Attainment of isotopic equilibrium between ocean water and the benthonic foraminifera genus *Uvigerina*: Isotopic changes in the ocean during the last glacial, *Colloq. Int. du CNRS*, *219*, pp. 203–210, Cent. Natl. de la Rech. Sci., Paris.

Shackleton, N. J., and N. D. Opdyke (1973), Oxygen isotope and palaeomagnetic stratigraphy of equatorial Pacific core V28–238: Oxygen isotope temperatures and ice volumes on a 100 kyrs and 1000 kyrs scale, *J. Quat. Res.*, *3*(1), 39–54.

Shackleton, N. J., M. F. Sánchez-Goñi, D. Pailler, and Y. Lancelot (2003), Marine Isotope Substage 5e and the Eemian Interglacial, *Global Planet. Change*, *36*, 151–155.

Thiede, J., and B. Junger (1992), Faunal and floral indicators of coastal upwelling (NW African and Peruvian Continental Margins), in *Upwelling Systems: Evolution Since the Early Miocene*, *Geol. Soc. Spec. Publ.*, edited by C. P. Summerhayes et al., *64*, 47–76.

Tuenter, E., S. L. Weber, F. J. Hilgen, and L. J. Lourens (2003), The response of the African summer monsoon to remote and local forcing due to precession and obliquity, *Global Planet. Change*, *36*, 219–235.

Vénec-Peyré, M.-T., and J.-P. Caulet (2000), Paleoproductivity changes in the upwelling system of Socotra (Somali Basin, NW Indian Ocean during the last 72,000 years: Evidence from biological signatures, *Mar. Micropaleontol.*, *40*, 321–344.

Vénec-Peyré, M.-T., J.-P. Caulet, and C. Vergnaud Grazzini (1995), Paleohydrographic changes in the Somali Basin (5°N upwelling and equatorial areas) during the last 160 kyr, based on correspondence analyses of foraminiferal and radiolarian assemblages, *Paleoceanography*, *10*(3), 473–492.

Vénec-Peyré, M.-T., J.-P. Caulet, and C. Vergnaud Grazzini (1997), Glacial/interglacial changes in the equatorial part of the Somali Basin (NW Indian Ocean) during the last 355 kyr, *Paleoceanography*, *12*(5), 640–648.

Vergnaud Grazzini, C., M. Devaux, and J. Znaidi (1986), Stable isotope "anomalies" in Mediterranean Pleistocene records, *Mar. Micropaleontol.*, *10*, 35–69.

Waelbroeck, C., L. Labeyrie, E. Michel, J. C. Duplessy, J. F. McManus, K. Lambeck, E. Balbon, and M. Labracherie (2002), Sea-level and deep water temperature changes derived from benthic foraminifera isotopic records, *Quat. Sci. Rev.*, *21*, 295–305.